

Misalignment of transverse anisotropies as a mechanism for suppression of Kondo effect in large spin single molecule magnets

Rui-Qiang Wang^{1,2,*} and D. Y. Xing¹

¹Department of Physics and National Laboratory of Solid State Microstructures, Nanjing University, Nanjing 210093, China

²Laboratory of Quantum Information Technology, ICMP and SPTE, South China Normal University, Guangzhou 510006, China

(Received 28 January 2009; published 28 May 2009)

The Kondo physics of a single molecule-magnet transistor is studied by taking into account the misalignment of magnetic axes of the molecule associated with different transverse anisotropies. It is shown that the misalignment of the transverse anisotropies strongly suppresses the Kondo temperature and even quenches it completely. The Kondo temperature exhibits a nonmonotonic behavior with respect to the strength of the transverse magnetic anisotropy and an oscillation behavior with the misaligned angle. We find that the interplay of different magnetization tunneling paths is essentially responsible for those behaviors. We suggest that elimination of the misaligned angle between axes is very important to observe the Kondo phenomenon experimentally.

DOI: [10.1103/PhysRevB.79.193406](https://doi.org/10.1103/PhysRevB.79.193406)

PACS number(s): 75.50.Xx, 72.10.Fk, 75.30.Gw, 75.45.+j

Measurements of electronic transport through individual magnetic molecule Mn_{12} acetate trapped in a nanogap^{1,2} have stirred great interest in single molecule-magnet (SMM) transistors,³⁻⁵ where the molecule with spin larger than $1/2$ is coupled to metallic leads. In the SMMs the intrinsic transverse anisotropy caused by spin-orbit effects results in quantum tunneling of magnetization (QTM), which tends to mix pairs of magnetic states with opposite spin projection separated by a strong easy-axis magnetic anisotropy. Detection of the fingerprints of QTM is helpful for shedding light on the physics of internal magnetic excitations. Recently, transport properties of the SMM transistor are suggested to provide an alternative signature, instead of usual magnetic relaxation time for an isolated SMM,⁶ to identify the QTM.^{1,2}

It is proposed that the SMM transistor is an ideal playground to explore large spin Kondo effect. It is well known that $1/2$ -spin Kondo effect in single molecule⁷ or single atom^{8,9} is a result of the flipping of local spin by a conduction electron. For a large spin SMM, however, the spin flipping is generally regarded to be hampered by the longitudinal anisotropy barrier. Only very recently, Romeike *et al.*¹⁰ suggest that the magnetization of SMMs can be reversed by allowing for the joint effect of spin exchange with electron reservoirs and the intrinsic transverse anisotropy, and hence the Kondo effect arises. They present a detailed analysis of the formation of the Kondo effect not only for the half-integer spin SMMs (Ref. 10) but also for the integer spin ones.^{11,12} This implies that the Kondo effect of SMMs might become a powerful tool to identify the QTM and understand its fundamental physics. Unfortunately, until now the Kondo effect in the SMMs has not been observed yet in despite of many experimental efforts. Theoretically, it is natural to ask if there are some unexpected causes which impede the formation of large spin Kondo physics mechanism mentioned above.

In the theoretical model for the SMM Kondo effect,¹⁰⁻¹⁴ multiplefold rotation symmetries of the transverse anisotropy need to be considered simultaneously. For instance, many evidences^{15,16} have confirmed that the transverse anisotropy of the Mn_{12} -acetate molecule is of a fourfold rotation sym-

metry. Meanwhile, the transverse anisotropy of a twofold rotation symmetry is imposed by disordered solvent molecules surrounding the magnetic core. Most interestingly, it has been reported that the in-plane (the plane perpendicular to the easy axis) principle axis of the second-order anisotropy deviates from that of the fourth order. In electron paramagnetic resonance experiments for Mn_{12} acetate, Barco *et al.*¹⁷ demonstrated a misaligned angle of as large as 30° between the hard axes, respectively, associated with the twofold and fourfold anisotropies. In the same system, Park *et al.*¹⁸ worked out a misaligned angle of 24° from the density-functional theory. This is acceptable because two types of anisotropies have different physics origins. The misaligned angle is so prominent that consideration of it is indispensable for some physical phenomena. Recently, a pioneering angle-dependent spin Hamiltonian,^{17,18} characterizing the incommensurate transverse anisotropies by a misaligned angle, is carried out. This spin Hamiltonian can be applied to explain many of experimental features¹⁷ and to predict that the oscillation of the tunnel splitting will be entirely quenched.¹⁸ However, so far there are yet no literatures devoted to the Kondo effect subject to the misalignment. This context gives us a great motivation to repredict the Kondo effect in the SMMs system beyond the previous considerations¹⁰⁻¹⁴ based only on the commensurate axes.

In this Brief Report, we study the Kondo effect for a SMM with misaligned magnetic axes associated with the second-order and fourth-order transverse anisotropy terms. Carrying out the similar analysis as in Ref. 10, we find that the misalignment of the transverse anisotropy suppresses the Kondo effect remarkably, even completely quenches it for some specific misaligned angles. Due to the rotation symmetry, the Kondo temperature exhibits an oscillation behavior with the misaligned angle. So, the misalignment probably is a key cause impeding the observation of the Kondo anomaly in the SMMs.

Let us consider an incommensurate spin Hamiltonian of SMMs coupled to two electron reservoirs

$$H = JS \cdot \mathbf{s} + \sum_{k\sigma} \varepsilon_{k\sigma} a_{k\sigma}^\dagger a_{k\sigma} - D_2 S_z^2 - D_4 S_z^4 - \frac{1}{2} B_2 [e^{-2i\alpha} S_+^2 + e^{2i\alpha} S_-^2] - \frac{1}{2} B_4 (S_+^4 + S_-^4), \quad (1)$$

where the first term stands for the spin-exchange coupling between the magnetic degrees of freedom \mathbf{S} of the SMM and the conduction-electron spin $\mathbf{s} = \sum_{k'l} \sum_{\sigma'\sigma} a_{k'l}^\dagger (\tau_{\sigma\sigma'}/2) a_{k'\sigma}$. Here, τ is Pauli spin matrix and operator $a_{k\sigma}^\dagger$ ($a_{k\sigma}$) creates (annihilates) an electron in leads with single-electron energy $\varepsilon_{k\sigma}$ and σ spin. The exchange coupling parameter $J > 0$ is of antiferromagnetic type due to large charge energy, which has been verified by González *et al.*¹⁴ making a second-order perturbative Schrieffer-Wolff transformation.¹⁹ The last two terms in upper line of Eq. (1) describe the second-order and fourth-order longitudinal magnetic anisotropies, whose eigenstate pairs $|\pm m\rangle$ with magnetic quantum number $|m| \leq S$ are energy degenerate. The z index is the spin projection along easy axis, chosen as z axis.

The last two terms in Eq. (1) are the second-order and fourth-order transverse anisotropy terms, which are, even though very weak, a key ingredient to give rise to the magnetization flipping between different magnetic states. S_\pm^2 (S_\pm^4) with spin raising operators $S_\pm = S_x \pm iS_y$ introduces additional spin-selection rule, only allowing the QTM to occur for m differing by 2 (4). It is emphasized that in Eq. (1), unlike previous spin Hamiltonian,¹⁰⁻¹⁴ we introduce an exponential prefactor $e^{\pm 2i\alpha}$ as a modification by taking into account the misalignment between principle axes of different transverse anisotropies. We choose the coordinates in the diagonal four-fold transverse anisotropic symmetry, and the hard axis of the twofold symmetry deviates that of the twofold symmetry by an angle α . This angle-dependent model Hamiltonian can be derived from the Hamiltonian in Refs. 17 and 18 by combining and neglecting the terms irrelevant to our subject. It is our start point to analyze the suppression of the Kondo effect.

Diagonalizing the full Hamiltonian in Eq. (1) in the space of magnetic states $|m\rangle$ with matrix elements $H_{m'm} = \langle m'|H|m\rangle$, we obtain its eigenstates. At low temperatures of interest here, the Kondo effect arises mainly from the spin flipping between energy-degenerate magnetic ground states $|\pm G\rangle$, while the excited state contribution is negligible. Define the pseudospin-1/2 operator in terms of the ground states as $P_x, iP_y = \frac{1}{2}(|+G\rangle\langle -G| \pm |-G\rangle\langle +G|)$ and $P_z = \frac{1}{2}(|+G\rangle\langle +G| - |-G\rangle\langle -G|)$. By using time-reversal symmetry and truncating the excited states, the system Hamiltonian can be mapped into an effective pseudospin-1/2 Kondo model,^{10,13}

$$H_{eff} = \sum_{i=x,y,z} J_i P_i s_i, \quad (2)$$

with effective exchange constants $J_{x,y} = J\langle +G|S_\pm \pm S_\mp|-G\rangle$ and $J_z = 2J\langle +G|S_z|+G\rangle$. Assumed a weak QTM $B_2(B_4) \ll D_2$, $J_{x,y}$ is far less than J_z exhibiting a strong anisotropy.¹³ It is noticed that except for the systemic parameters B_2 and B_4 , the angle α also enters into $J_{x,y}$ and J_z to modify the exchange coupling strengths. In order to examine the strong

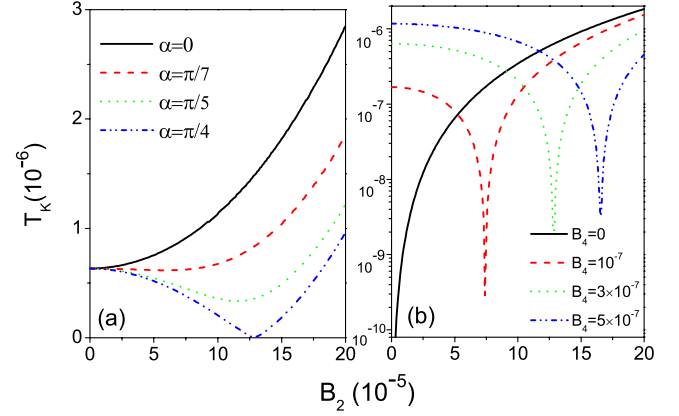


FIG. 1. (Color online) Kondo temperature T_K curves as functions of parameter B_2 for (a) indicated misaligned angles and $B_4 = 3 \times 10^{-7}$ for (b) indicated parameters B_4 and $\alpha = \pi/4$. The other parameters are $J = 0.1$, $D_2 = 5 \times 10^{-3}$, $D_4 = 0$, and $s = 5/2$.

anisotropic Kondo effect, it is convenient to employ Poorman scaling laws,²⁰ which was once applied to predict the splitting of zero-bias Kondo peak²¹ in an individual C_{60} molecule coupled to two ferromagnetic leads. This prediction is in well agreement with afterwards experiment.²² Again, it is extensively applied for analysis of the Kondo effect in the SMM transistor.^{10,12-14} Here, we adopt the same method and express the flow equations to renormalize the effective exchange couplings as^{10,13} $\frac{dJ_{xy}}{d\xi} = -\rho J_{y,x} J_z$ and $\frac{dJ_z}{d\xi} = -\rho J_x J_y$, where ρ is density of states and $\xi = \ln(\tilde{W}/W)$ with half bandwidth W being rescaled as \tilde{W} . As a result, all coupling constants reach a stable strong-coupling fixed point at the Kondo energy scale, $|J_x| = |J_y| = |J_\perp|$ and $J_z^2 - J_\perp^2 = \text{const}$. The corresponding Kondo temperature can be defined as

$$\ln(T_K/\Delta E) = -\frac{\text{arctanh}[\sqrt{J_z^2 - J_\perp^2}/J_z]}{\rho \sqrt{J_z^2 - J_\perp^2}}, \quad (3)$$

where ΔE is the energy difference between the ground state and the first-excited state.

In Fig. 1(a), we plot the Kondo temperature T_K as functions of the second-order anisotropy parameter B_2 for different misaligned angles α . Take W as a unit of energy. For the commensurate principle axes of $\alpha = 0$ (solid line), T_K is enhanced monotonically with B_2 increasing, which is in agreement with the previous results¹⁰ in the regime of small B_2 . But for the nonzero α , T_K is evidently suppressed which becomes more and more strong with α increasing. Furthermore, for large α , T_K exhibits a nonmonotonic behavior. Especially when $\alpha = \pi/4$, a dip arises at certain B_2 , at which the corresponding Kondo effect is completely quenched. Even though one reinforces fourth-order anisotropy parameter B_4 , the Kondo dip still persists as long as the principle axes of the anisotropies are misaligned. This result can be seen in Fig. 1(b), which gives the variations in the Kondo temperature vs B_4 for a fixed angle $\alpha = \pi/4$. Increasing B_4 can only delay the appearance of the dip but cannot smear it away. As a limit of $B_4 = 0$, the dip is at $B_2 = 0$, regardless of the angle α ,

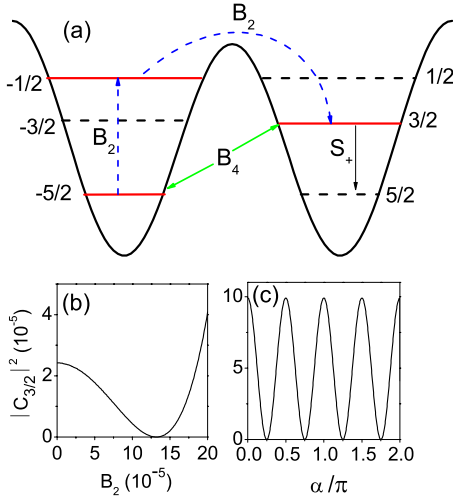


FIG. 2. (Color online) (a) Scheme of anisotropy barrier with $s=5/2$: a high longitudinal anisotropy spacing opposite spin states and transverse anisotropies connecting them selectively. Probability $|C_{3/2}|^2$ at state $|3/2\rangle$ as a function of (b) B_2 and (c) α at the dip in Fig. 1(a).

due to no available QTM. Therefore, the principle axes misalignment might become a great obstacle for observation of the Kondo effect.

Understanding of the Kondo behaviors mentioned above is closely involved the internal magnetic state reversal. In Fig. 2(a), we plot the classic longitudinal anisotropy barrier which separates the magnetic states with antiparallel orientation of the spin z projection. The QTM stems from the transverse anisotropies B_2 and B_4 , which allow the transitions between different magnetic states but obey specific spin-selection rule, changing the magnetic number m by 2 for B_2 and 4 for B_4 . Thus, the system establishes two sets of independent subspaces for $s=5/2$: $\{|-5/2\rangle, |-1/2\rangle, |3/2\rangle\}$ and $\{|5/2\rangle, |1/2\rangle, |-3/2\rangle\}$, whose linear combination with the lowest energy forms into two degenerate ground states $| -G\rangle$ and $| +G\rangle$, respectively, in each subspace. At low temperature, the Kondo effect is a consequence of the spin flipping between the ground-state doublets $|\pm G\rangle$ by a conduction electron, e.g., $|3/2\rangle \rightarrow |5/2\rangle$ by S_+ . The prerequisite to ensure this process is that there is nonzero occupation probability $|C_{3/2}|^2$, where $C_{3/2}$ is the probability amplitude of the ground state $| -G\rangle$ in the magnetic state $|3/2\rangle$. $|C_{3/2}|^2$ is determined by the magnetization transition between $| -5/2\rangle$ and $|3/2\rangle$, which has two paths owing to two kinds of transverse anisotropies, namely, $| -5/2\rangle \rightarrow |3/2\rangle$ governed by B_4 and $| -5/2\rangle \rightarrow |-1/2\rangle \rightarrow |3/2\rangle$ governed by B_2 , as depicted in Fig. 2(a). For commensurate transverse anisotropies, the overriding of the hard axes associated with B_2 and B_4 is favorable for opening of two channels above at the same time, and hence the T_K monotonically increases with B_2 [see Fig. 1(a)]. On the contrary, for incommensurate configuration, we find that the nonmonotonic behavior of T_K in Fig. 1(a) is determined by nonmonotonic $|C_{3/2}|^2$. In Fig. 2(b) we plot its behavior as a function of B_2 for $\alpha = \pi/4$, where the hard axis of the twofold symmetry just superposes the mediate axis of the fourfold one (refer to Ref. 17). In this configuration, $|C_{3/2}|^2$ reduces firstly with increasing B_2 due to relatively weak tran-

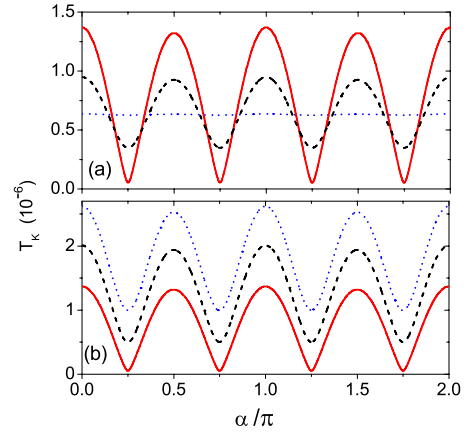


FIG. 3. (Color online) Kondo temperature T_K curves as functions of misaligned angle α , (a) for $B_2=0.5 \times 10^{-5}$ (dotted line), $B_2=10^{-5}$ (dashed line), and $B_2=2 \times 10^{-5}$ (solid line) with $B_4=3 \times 10^{-7}$; (b) for $B_4=3 \times 10^{-7}$ (solid line), $B_4=5 \times 10^{-7}$ (dashed line), and $B_4=7 \times 10^{-7}$ (dotted line) with $B_2=2 \times 10^{-5}$. The other parameters are the same as in Fig. 1.

sition $| -5/2\rangle \rightarrow |3/2\rangle$ when the transition $| -5/2\rangle \rightarrow |-1/2\rangle$ becomes accessible but the next process $|-1/2\rangle \rightarrow |3/2\rangle$ is quite weak for small B_2 . If the B_2 increases further, both the channels governed by B_2 and B_4 open and thereby the probability $|C_{3/2}|^2$ increases quickly. The nonmonotonic behavior of $|C_{3/2}|^2$ becomes very visible for larger α . However, when α is greater than $\pi/4$, $|C_{3/2}|^2$ shows an $\pi/4$ -periodic function due to the symmetry, as presented in Fig. 2(c).

In Fig. 3, we present the Kondo temperature T_K as functions of the misaligned angle α (a) for different B_2 and (b) for different B_4 . As is expected, there is a well-defined oscillatory curve of the Kondo temperature T_K , corresponding to the fourfold rotation symmetry with the maximum at $\alpha = n\pi/2$ ($n=0, \pm 1, \pm 2, \dots$) and the minimum at $\alpha = n\pi/2 + \pi/4$. If the B_2 is weak, as plotted in horizontal dot line in Fig. 3(a), the misalignment effect can be negligible since the T_K almost remains a constant, which is determined by the channel associated with B_4 . For large B_2 , however, the misalignment plays an important role. With B_2 increasing, T_K oscillates around the fixed constant and the oscillation amplitude becomes larger and larger. This is because B_2 can enhance or reduce the probability in the state $|3/2\rangle$, dependent on the misaligned angle, by modulating the transition channel $| -5/2\rangle \rightarrow |-1/2\rangle \rightarrow |3/2\rangle$. In the Fig. 3(b), we exhibit the oscillatory dependence of T_K on different parameters B_4 . When B_4 becomes large, the curves is lifted higher or the Kondo temperature T_K increases but the oscillation behavior with α remains unchanged. The B_4 -enhanced Kondo temperature is as a consequence of enhancing the direct coupling between states $| -5/2\rangle$ and $|3/2\rangle$.

We also examine the integer spin SMMs, in which the Kondo effect under consideration involving only the ground state vanishes. However, s mixing²³ involving high-lying spin multiplets will make the Kondo effect recover,¹¹ and α -induced suppression is still expected as long as there exists the misalignment because of the existence of the destructive interference between different magnetization tunneling paths for the two types of anisotropies.

In summary, we have investigated the Kondo effect in a SMM transistor, where the magnetic axes of the SMM associated with the second- and fourth-order transverse anisotropies are incommensurate. Taking half-integer spin SMM $s = 5/2$ as an example, we find that the misalignment of the transverse anisotropies strongly suppresses the Kondo temperature and even completely quenches it. For large misaligned angle, a nonmonotonic dependence on the strength of the transverse magnetic anisotropy of the molecule is shown. Furthermore, the Kondo temperature exhibits an oscillation behavior vs the misaligned angle. The underlying physics is the interference between different magnetization tunneling

paths. These results suggest that in order to observe the Kondo effect best experimentally, one should apply, e.g., mechanical or chemical methods, to manipulate the solvent molecules surrounding the magnetic core and so lessen the misaligned angle between axes of different transverse anisotropies.

This work was supported by the National Natural Science Foundation of China under Grants No. 90403011 and No. 10874066 and also by the State Key Program for Basic Researches of China under Grants No. 2006CB921803, No. 2004CB619004, 2007CB925104, and No. 2009CB929504.

*rqwanggz@163.com

- ¹H. B. Heersche, Z. de Groot, J. A. Folk, H. S. J. van der Zant, C. Romeike, M. R. Wegewijs, L. Zobbi, D. Barreca, E. Tondello, and A. Cornia, *Phys. Rev. Lett.* **96**, 206801 (2006).
- ²M. H. Jo, J. E. Grose, K. Baheti, M. M. Deshmukh, J. J. Sokol, E. M. Rumberger, D. N. Hendrickson, J. R. Long, H. K. Park, and D. C. Ralph, *Nano Lett.* **6**, 2014 (2006).
- ³L. Bogani and W. Wernsdorfer, *Nature Mater.* **7**, 179 (2008).
- ⁴M. Misiorny and J. Barnaś, *Phys. Rev. B* **76**, 054448 (2007).
- ⁵C. Timm and F. Elste, *Phys. Rev. B* **73**, 235304 (2006).
- ⁶D. Gatteschi, R. Sessoli, R. Sessoli, and D. Gatteschi, *Angew. Chem., Int. Ed.* **42**, 268 (2003).
- ⁷W. Liang, M. P. Shores, M. Bockrath, J. R. Long, and H. Park, *Nature (London)* **417**, 725 (2002).
- ⁸J. Park, A. N. Pasupathy, J. I. Goldsmith, C. Chang, Y. Yaish, J. R. Petta, M. Rinkoski, J. P. Sethna, H. D. Abruna, P. L. McEuen, and D. C. Ralph, *Nature (London)* **417**, 722 (2002).
- ⁹A. F. Otte, M. Ternes, K. V. Bergmann, S. Loth, H. Brune, C. P. Lutz, C. F. Hirjibehedin, and A. J. Heinrich, *Nat. Phys.* **4**, 847 (2008).
- ¹⁰C. Romeike, M. R. Wegewijs, W. Hofstetter, and H. Schoeller, *Phys. Rev. Lett.* **96**, 196601 (2006).
- ¹¹C. Romeike, M. R. Wegewijs, W. Hofstetter, and H. Schoeller, *Phys. Rev. Lett.* **97**, 206601 (2006).
- ¹²M. R. Wegewijs, C. Romeike, H. Schoeller, and W. Hofstetter, *New J. Phys.* **9**, 344 (2007).
- ¹³M. N. Leuenberger and E. R. Mucciolo, *Phys. Rev. Lett.* **97**, 126601 (2006).
- ¹⁴G. González, M. N. Leuenberger, and E. R. Mucciolo, *Phys. Rev. B* **78**, 054445 (2008).
- ¹⁵A. Cornia, R. Sessoli, L. Sorace, D. Gatteschi, A. L. Barra, and C. Daugebonne, *Phys. Rev. Lett.* **89**, 257201 (2002).
- ¹⁶S. Hill, R. S. Edwards, S. I. Jones, N. S. Dalal, and J. M. North, *Phys. Rev. Lett.* **90**, 217204 (2003).
- ¹⁷E. del Barco, A. D. Kent, S. Hill, J. M. North, N. S. Dalal, E. M. Rumberger, D. N. Hendrickson, N. Chakov, and G. Christou, *J. Low Temp. Phys.* **140**, 119 (2005).
- ¹⁸K. Park, M. R. Pederson, T. Baruah, N. Bernstein, J. Kortus, S. L. Richardson, E. del Barco, A. D. Kent, S. Hill, and N. S. Dalal, *J. Appl. Phys.* **97**, 10M505 (2005).
- ¹⁹J. R. Schrieffer and P. A. Wolff, *Phys. Rev.* **149**, 491 (1966).
- ²⁰P. W. Anderson, *J. Phys. C* **3**, 2436 (1970).
- ²¹J. Martinek, Y. Utsumi, H. Imamura, J. Barnaś, S. Maekawa, J. König, and G. Schön, *Phys. Rev. Lett.* **91**, 127203 (2003).
- ²²A. N. Pasupathy, R. C. Bialczak, J. Martinek, J. E. Grose, L. A. K. Donev, P. L. Mceuen, and D. C. Ralph, *Science* **306**, 86 (2004).
- ²³S. Carretta, E. Livioti, N. Magnani, P. Santini, and G. Amoretti, *Phys. Rev. Lett.* **92**, 207205 (2004).